Step-by-Step Design of a LLC Resonant Converter for EV Fast Charging Applications

Joao Rocha
University of Minho
ALGORITMI / LASI
Guimaraes, Portugal
pg50485@alunos.uminho.pt

Saghir Amin
University of Minho
ALGORITMI / LASI
Guimaraes, Portugal
id11315@alunos.uminho.pt

Goncalo Rego
University of Minho
ALGORITMI / LASI
Guimaraes, Portugal
pg50403@alunos.uminho.pt

Joao L. Afonso
University of Minho
ALGORITMI / LASI
Guimaraes, Portugal
jla@dei.uminho.uminho.pt

Vitor Monteiro
University of Minho
ALGORITMI / LASI
Guimaraes, Portugal
vmonteiro@dei.uminho.pt

***Abstract* — Electric mobility is already well established in societies, but there are still several technological challenges to overcome. Specifically, a key challenge is the concern about charging systems, which should be faster and more efficient. In this context, regarding the DC-DC back-end power stage, a special emphasis is given to LLC resonant power converters. Aligned with this context, this paper presents a step-by-step design and description of a LLC resonant power converter. MATLAB and PSIM simulation models were developed for validating, respectively, the gain design of the LCC tank and the analysis of the operation considering such different designs. For validation purposes, an input voltage of 900 V, an output voltage of 900 V, and a resonant frequency of 100 kHz were considered. The validating results were obtained for different conditions of operation, according to the different designs, showing a maximum estimated efficiency of 99.5%.**

Keywords—**Electric Mobility, Power Electronics, LLC Resonant Converter.**

I. INTRODUCTION

Electric mobility is recognized as portraying a revolutionary and transformative shift in transportation paradigm, offering manifold benefits in terms of reducing greenhouse gas emissions in urban areas toward a more sustainable solution of mobility [1]. Thus, in addition of the inherent technological advances when contextualized with smart grids [2], it also represents a contribution for the societal and environmental evolution.

Concerning the adoption of electric vehicles (EV) as a new way of transportation, a set of additional technologies also have to be thought of, like battery technology, its advancements, and the charging infrastructure, which can influence the design of cities regarding the strategic position of EV charging stations [3]. For the massive adoption of EV, it is well identified that EV charging stations are the vital arteries of the electric mobility ecosystem, offering the indispensable convenience and accessibility to the EV owners. As the demand for EV rises, the increase of EV charging infrastructures must become dominant, requiring dedicated power management strategies [4]. Regarding charging systems, with the advancements in power electronics technologies, EV fast charging stations are becoming commonplace, offering the possibility of drastically reducing the charging times [5]. Moreover, it also contributes to enhance the practicality of EV for daily use.

For implementing EV fast charging stations, several topologies of power electronics systems can be adopted, including three-phase interleaved-based topologies [6]. In fact, power electronics is the core of EV charging stations, and the adoption of innovative topologies is of paramount importance since it plays a pivotal role in optimizing charging efficiency and managing the interaction with the power grid [7]. From established AC charging (on-board or off-board) to advanced DC fast charging systems (off-board), diverse topologies satisfy to different charging needs [8]. Specifically, AC-DC diode bridge rectifiers and DC-DC boost-type and buck-type converters are commonly used, respectively as front-end and back-end power conversion, transforming the AC power grid variables of voltages and currents into DC voltage and current for charging the EV batteries [9]. Concerning the galvanic isolation between the power grid and the EV battery, some common topologies can be employed like full-bridge or half-bridge (i.e., denominated dual active bridge topologies), also offering the possibility of operating with different voltage levels in both sides of the converter and, if necessary, in bidirectional mode. Independently of the topology, the final objective is to minimize the charging time without compromising EV battery health [10].

In this context, a step-by-step design and description of a LLC resonant power converter is presented in this paper for EV fast charging applications. To accomplish with such objective, a MATLAB simulation model was developed, where the maximum input and output voltages were fixed, respectively, in 900 V and 900 V. The resonant frequency was 100 kHz. The distinguished points of this paper are: (i) step-by-step design of a LLC resonant power converter, from the simulations to a laboratorial prototype; (ii) analysis for different case studies; (iii) investigation regarding the estimated efficiency based on the EV fast charging operating power; (iv) estimation of losses distribution.

II. LLC RESONANT CONVERTER: ANALYSIS OF THE DESIGN

The initial concept of a resonant converter consisted of incorporating resonant tanks into the power converters to create oscillatory voltage and/or current waveforms, allowing conditions to be created for zero voltage or zero current

switching. This makes possible the reduction of the switching losses due to the soft switching. Specifically, LLC resonant converters become a good option for EV fast charging applications, since using the ZVS and ZCS soft switching techniques, it is possible to increase the value of the switching frequency and at the same time reduce the power density, thus making the converter more efficient [11].

A. LLC Resonant Converter Design

The LLC resonant converter under study in this paper consists of four different stages, as shown in Fig. 1. The first stage is the full-bridge inverter composed by four power switching devices, which can achieve a square waveform with an amplitude of voltage, whose values correspond to the value of the input voltage, and a frequency defined by the switching frequency. The second stage is the resonant tank, composed by a series of inductance (L_r) and a capacitor (C_r), and a shunt inductance (L_m) with the primary side of the HFT. The third stage corresponds to the full-wave diode rectifier. The fourth stage is the output capacitor (C_o), which is used for ensuring an output voltage with low ripple.

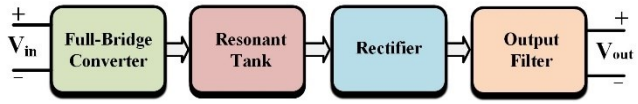

Fig. 1. Block diagram of the LLC resonant converter.

Besides these four stages, it also includes a HFT to ensure galvanic isolation between the input and output. Based on the design, it is also possible to adjust the voltage using the transformation ratio. The LLC resonant converter is presented in Fig. 2. It permits the operation in three different modes with different resonant frequencies. The operation of the LLC resonant converter with a frequency higher than the resonant frequency is used for achieving zero voltage switching (ZVS), which is in delayed power factor mode. On the other hand, the operation of the LLC resonant with a frequency lower than de resonant frequency is used for achieving zero current switching (ZCS), which is in advanced power factor mode. Finally, with the operation of the LLC resonant converter with the same frequency of the resonant frequency is not achieved ZVS or ZCS. Therefore, for EV fast charging applications, it is expected the operation of the LLC resonant converter with a frequency above the resonance frequency, allowing to achieve higher efficiency and stability [12].

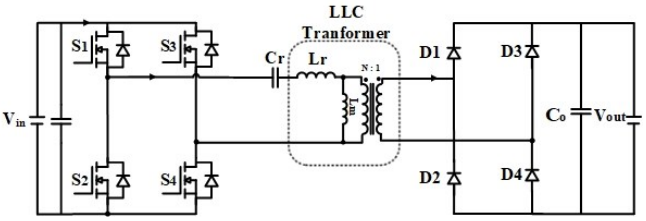

Fig. 2. Topology of the LLC resonant converter under study in this paper.

The LLC resonant converter has two distinct frequencies that can be calculated by (1) and (2) [12]-[15]:

$$f_{r1} = \frac{1}{2\pi\sqrt{L_r * C_r}}, \tag{1}$$

$$f_{r2} = \frac{1}{2\pi\sqrt{(L_r + L_m) * C_r}}. \tag{2}$$

The equivalent load resistance circuit, which depends on the transformation ratio, is given by (3):

$$R_{ac} = \frac{8\, n^2\, R_{out}}{\pi^2}. \tag{3}$$

The quality factor (Q) of the LLC resonant converter is calculated using (4):

$$Q = \frac{\sqrt{L_r/C_r}}{R_{ac}}. \tag{4}$$

The normalized frequency is calculated by (5):

$$f_n = \frac{f_{r2}}{f_{r1}} \tag{5}$$

The relationship between the two inductances is given by (6):

$$m = \frac{L_r + L_m}{L_r}. \tag{6}$$

Finally, in the equivalent circuit of the LLC resonant converter with a non-ideal transformer, the ratio between the output and the input voltage corresponds to the gain of the resonant circuit, which is given by (7):

$$G_d = \frac{V_{Rdc}}{V_{in}} = \left| \frac{\left(\frac{f^2}{{f_{r1}}^2}\right) * \sqrt{m(m-1)}}{\left(\frac{f}{{f_{r2}}^2} - 1\right) + j\frac{f}{{f_{r1}}^2}\left(\frac{f^2}{{f_{r1}}^2} - 1\right)(m-1)Q} \right|. \tag{7}$$

B. Effect of the Quality Factor and Power

To evaluate the performance of the resonant tank, two tests were carried out considering five combinations of values of the L and C elements that make it up. In the first test, the value of the quality factor was fixed to verify how it affects the gain of the LLC resonant converter. In the second test, it was considered a variation of the load resistance to verify the maximum gain for various output power values. The five cases considered for the study are as presented in Table I and they were chosen so that it would be possible to have a reasonable range of values to combine the simulation and obtain the best possible result and choose the most plausible values to reproduce in real life.

TABLE I. LLC RESONANT CONVERTER CASE STUDIES

	Cr	Lr	Lm
case 1	800 nF	3 µH	200 µH
case 2	480 nF	5 µH	200 µH
case 3	340 nF	7 µH	200 µH
case 4	265 nF	9 µH	200 µH
case 5	218 nF	11 µH	200 µH

It is possible to see some changes over the five case studies due to the impact of the quality factor on the resonant tank. The analysis was carried out using the MATLAB software to simulate and verify the influences of the gain curves. As can

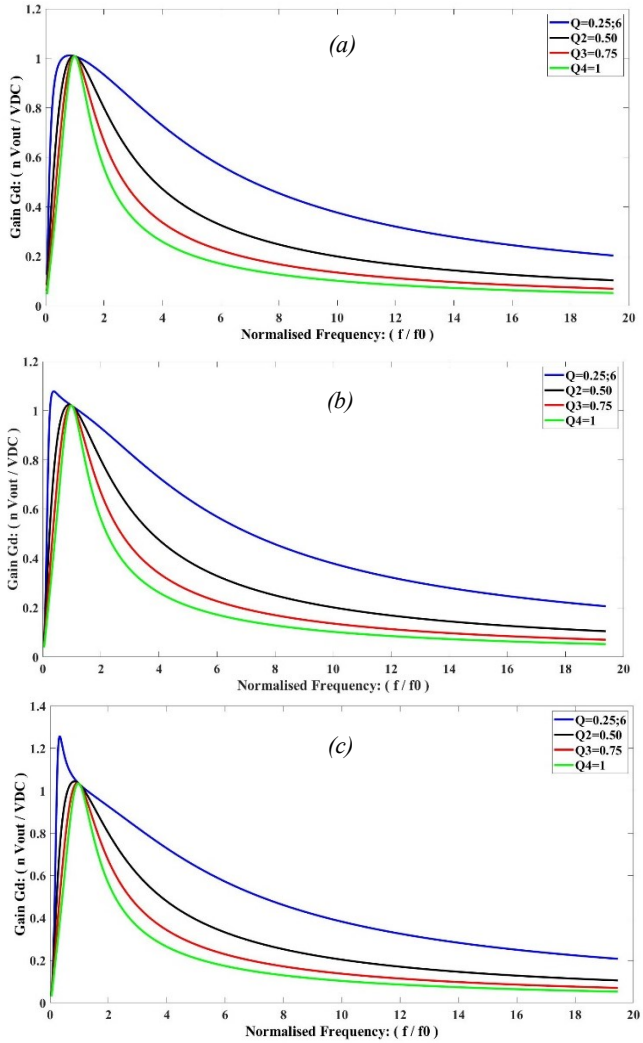

Fig. 3. Q effect on the LLC resonant converter considering three different cases: (a) case 1;(b) case 3; (c) case 5.

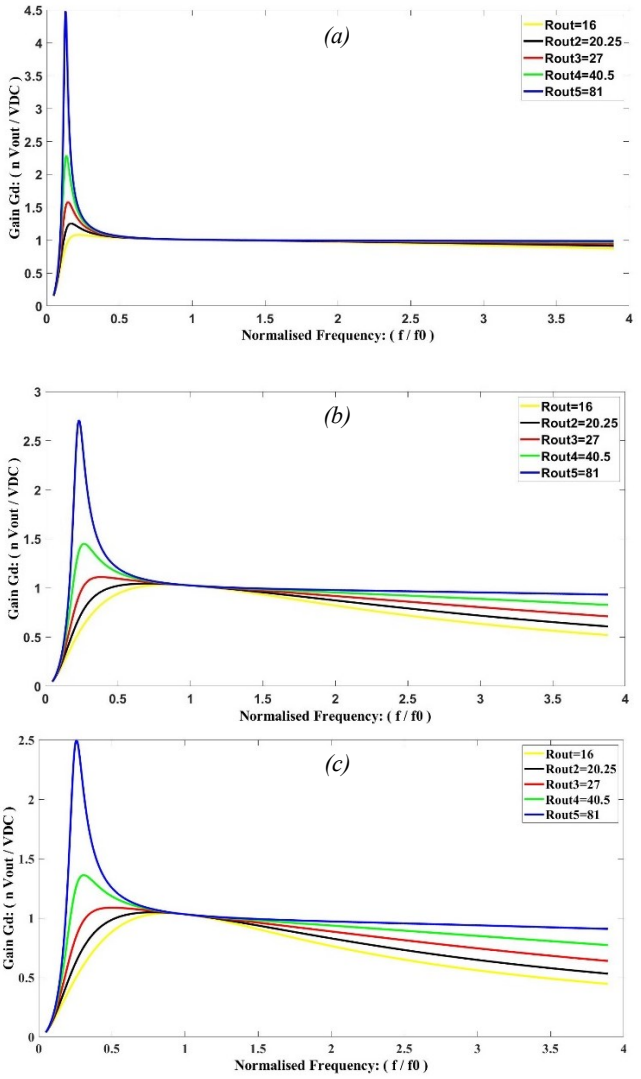

Fig. 4. Output load effect on the converter considering three different cases: (a) case 1; (b) case 3; (c) case 5.

be verified in Fig. 3 three graphs corresponding to case one, three and five respectively.

Throughout the analysis of the obtained results, it is possible to see that the maximum gain is influenced by the value of the quality factor, which is higher when the quality factor is lower but, at the same time, it is also influenced by the values used in the components of the resonant tank. In turn, the normalized frequency at the point of unitary gainer is also dependent on the component values, but these values do not vary with the quality factor imposed in each situation. Considering the analysis done on the second study, it was investigated the influence of the load resistance value. To do this, the desired power output was changed using 10 kW, 20 kW, 30 kW, 40 kW and 50 kW for the following resistance values 51 Ω, 40.5 Ω, 27 Ω, 20.25 Ω and 16 Ω, respectively. The results obtained for the three previous case studies can be checked in Fig. 4.

Analyzing these three graphs, it is possible to verify some differences, but there is one key point where this analysis focused, which is on the influence of the change of power on frequency. At the unitary gain point, the higher the frequency range, the better is the system behavior, which is verified in the first case study, where the frequency ranges from 70 kHz to 140 kHz, unlike case study five, where the range is substantially smaller. In addition to the abovementioned, it is again clear that there is a variation in gain in each of these cases, demonstrating once again that it is necessary to achieve a balance between all the parameters, i.e., component value, system gain and time interval between frequencies. After this analysis, the best sets of values can be selected to be used in the simulation process and then to be adjusted to the real values. Although the first case study gives the best results, it would be impossible to find or produce an inductance with that value, thus, it was opted for the second case study (confirm Fig. 5), which gives similar results and would be easier to reproduce when making a laboratorial prototype.

III. ADVANTAGES OF THE LLC RESONANT CONVERTER

Compared to other DC-DC converter topologies, the LLC resonant converter has a significant number of advantages, demonstrating that its use is beneficial when used in applications such as EV fast chargers. Increasing the switching frequency to values above 100 kHz will result in a reduction of the power density of the converter, which will consequently result in a reduction in the size of the converter and therefore of the charging station. The LLC resonant converter also solves the problem of switching losses by

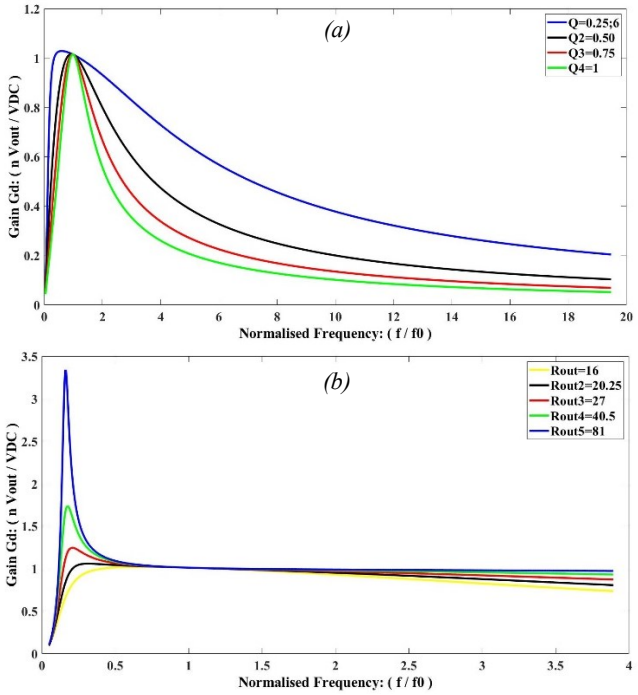

Fig. 7. Case study 5 defined as the best scenario: (a) Q effect (b) power effect.

making this process more efficient through the ZVS and ZCS control technique. In addition, it provides galvanic isolation between the input and output, which is offered by the high-frequency transformer present in the circuit. These advantages make the EV fast charger not only more efficient, but also more cost-effective compared to other available design options. Summarizing, the main advantages are increased switching frequency; decreased power density; galvanic insulation; increased efficiency; cost reduction [16].

IV. Computer Simulations of the LLC Resonant Converter

A. Current and Voltage Variation

With the objective of understand the five previous study cases, some introductory simulations were carried out, permitting to comprehend how the variation of the resonance inductance and its capacitor affect the behavior of the system [17][18]. The two important points to realize initially are how voltage and current are affected by the alternation of these values. Fig. 6 shows the voltage variation for the three-case study, where it is possible to understand that exist some changes in each case. If the capacitor value its increased, the peak voltage passing through the resonant tank decreases. The value obtained for case 1 is in the region of 87 V and with the capacitor reduced to 218 nF, the output voltage is around 300 V. On the other hand, after checking the current in these same three study cases, it was possible to see that by varying the values of the capacitor and the resonance inductance there was no drastic change in the value of the current passing through the resonant tank, i.e., there was no influence on the system, as can be seen in Fig. 7. In addition to these two initial tests, it is possible to start to visualize the appearance of the ZVS and ZCS control [19], which is adjusted due to the value of the magnetizing inductance, as presented in Fig. 8. With this, it is possible to start to get a full view of the system behavior and which components to

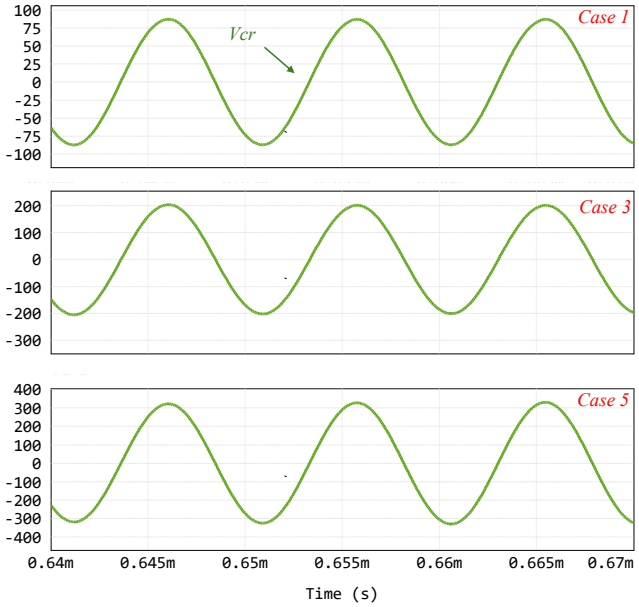

Fig. 5. Voltage variation in different case studies: (a) case 1 with peak voltage value equal to 87 V; (b) case 3 with peak voltage value equal to 205 V;(c) case 5 with peak voltage value equal to 318 V.

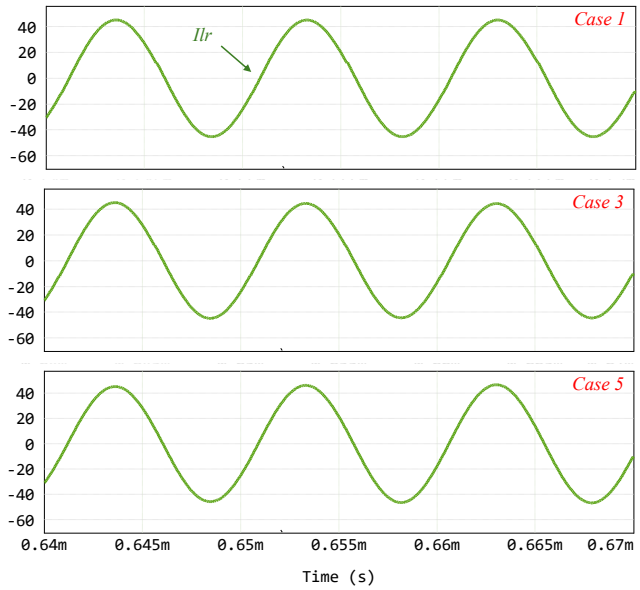

Fig. 6. Current variation in different case studies: (a) case 1 with peak current value equal to 44 A; (b) case 3 with peak voltage value equal to 44.2 A ;(c) case 5 with peak voltage value equal to 44.3 A.

use. Firstly, it was realized that increasing the value of the inductance coil, reduces the frequency range, which can make it a easier to obtain a real value for the transformer output. Secondly, increasing the values of the capacitor is not advantageous for the system, as it will represent a substantial increase in the voltage value, and lastly, it is also clear that the peak current value will not change a lot with these variations. It is now possible to achieve a final solution when moving to the real laboratorial prototype.

B. Output and Input Waveforms

In order to better understand how the converter works, there is also the need to know the voltage and current waveforms at the input and output of the converter. Bearing in mind that the LLC resonant converter is a DC-DC converter, a continuous signal is expected at the input and output in this

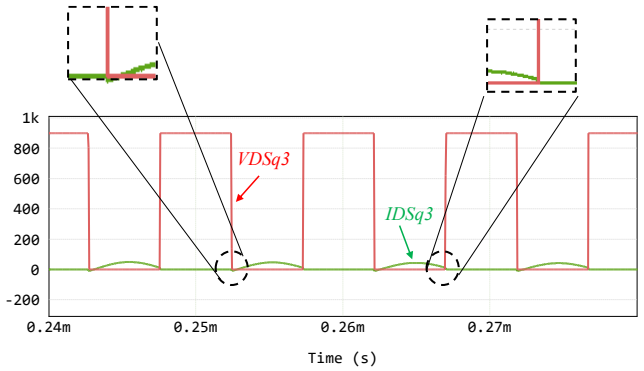

Fig. 12. Detail of the ZVS and ZCS operation on the MOSFET G3R30MT12J (cf. MOSFET s_3 in Fig. 2), considering an operating power of 25 kW, a voltage of 900 V, and a frequency of 100 kHz.

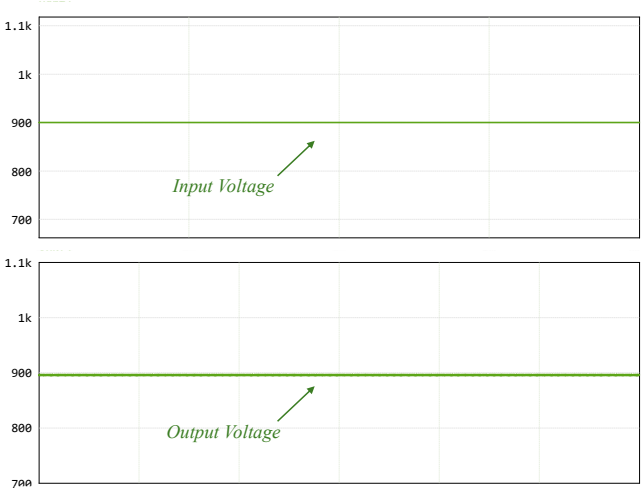

Fig. 13. Waveforms: (a) input voltage with 900 V; (b) Output voltage with 900 V.

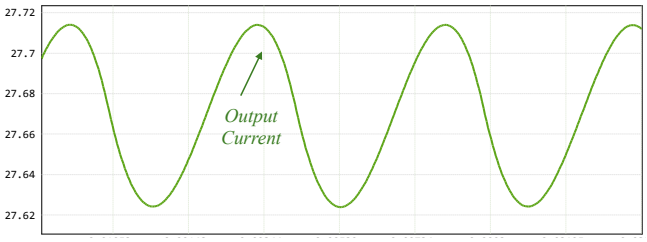

Fig. 14. Waveforms output current with 27.7 A peak.

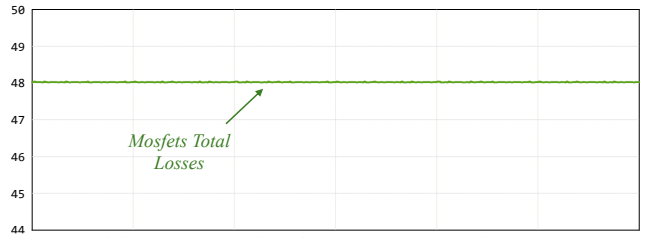

Fig. 8. Total losses associated to the MOSFETs, considering an operating power of 25 kW and a voltage of 900 V.

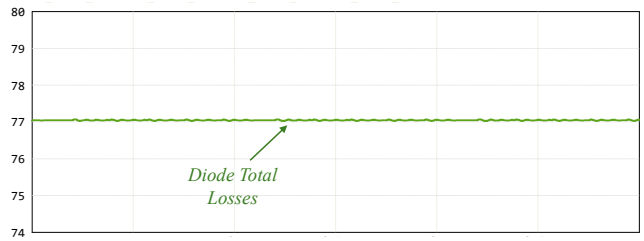

Fig. 9. Total losses associated to the diodes, considering an operating power of 25 kW and a voltage of 900 V.

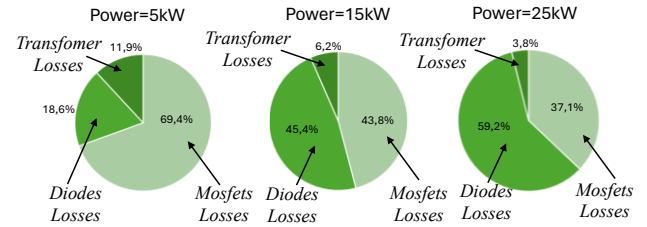

Fig. 10. Power losses distribution considering the high-frequency transformer, the diodes and the MOSFETs and a power range from 5 kW to 25 kW.

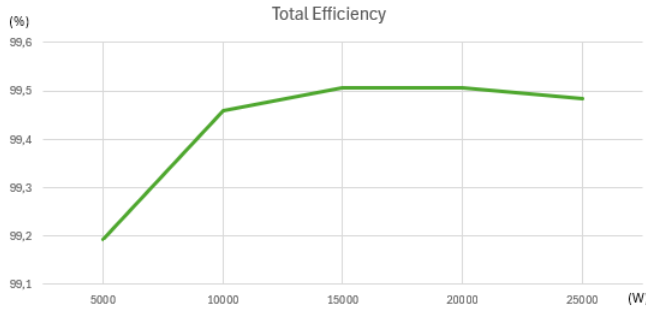

Fig. 11. Estimated efficiency considering a power range from 5 kW to 25 kW.

case with a value of 900V since the transformer has a ratio of one to one, as shown in Fig. 9. On the other hand, the presence of a sinusoid at the output of the converter is to be expected, as presented in Fig. 10.

C. Converter Losses

It is possible to simulate the losses of the entire circuit [8], i.e. the switching losses in the Mosfets, the losses in the diodes and finally the losses in the transformer. The PSIM tool was used to simulate the losses and two components were chosen that could be used as MOSFET and with diodes. Losses were calculated for all the previous case studies, but to understand them better, only case study 1 at a nominal power of 25 kW was presented. Regarding the calculations of the losses in the MOSFETs, it is possible to see in Fig. 11 that they have a value of around 46 W. In addition to this value, the diode losses were also calculated, giving a rounded value of 78.1 W, as shown in Fig. 12. Finally, in addition to these two values, it is also necessary to consider the value of the losses in the high-frequency transformer. To do this, MATLAB was used as well as some additional equations to reach a transformer losses value of around 4.98 W. Thus, the values of the total losses for case study one is around 128 W, which represents an efficiency of about 99.4%.

The graphs in Fig. 13 show the influence of power variation on the losses related to each component. It is clear that the component that suffers the most changes is the diode, while the losses in the transformer remain almost unchanged. With this, it is possible to identify where greater attention needs to be paid to when choosing components and how they are used to optimize the system as much as possible. This made it possible to draw the final graph of the system's efficiency [20], as presented in Fig. 14. It should also be noted that these losses do not change when the case under study is altered.

V. CONCLUSION

In the perspective of the design and development of a LLC resonant converter, it is necessary to go through several stages and fully understand how these work in different design conditions. So, from defining the gain equation, including all the step-by-step involved equations, to calculating the total losses of the converter, there is a path to follow where the path is as follows. In a first step, it was realized how the converter works in blocks, i.e., to understand how each stage works. After that, it was calculated the gain equation for the selected frequencies and the best combination of resonant capacitor and resonant coil was determined using the gain curves, permitting to analyze two different parameters, namely the Q factor and the power. Following, it was considered how current and voltage are affected through computer simulations and verified the occurrence of ZVS and ZCS operation (i.e., how it varies with the value of L_m). After that, based on the PSIM simulation model, it was performed an analysis concerning the estimated efficiency. After completing all of these steps, regarding a laboratorial prototype, additional challenges will arise in terms of hardware, namely finding a balance between the *Cr* and *Lr* values, allowing the design optimization of transformer.

ACKNOWLEDGMENT

This work has been supported by FCT – Fundação para a Ciência e Tecnologia within the R&D Units Project Scope: UIDB/00319/2020.

REFERENCES

[1] T. Ercan, N. C. Onat, N. Keya, O. Tatari, N. Eluru, and M. Kucukvar, "Autonomous electric vehicles can reduce carbon emissions and air pollution in cities," Transp Res D Transp Environ, vol. 112, Nov. 2022, doi: 10.1016/j.trd.2022.103472.

[2] V. Monteiro, J. A. Afonso, J. C. Ferreira, and J. L. Afonso, "Vehicle electrification: New challenges and opportunities for smart grids," Energies (Basel), vol. 12, no. 1, Jan. 2019, doi: 10.3390/en12010118.

[3] Parvathy. R. Professor, "Battery Charging Systems," Journal of Applied Science, Engineering, Technology and Management, vol.1, no.1, pp.33-38, June 2023.

[4] F. Lo Franco, V. Cirimele, M. Ricco, V. Monteiro, J. L. Afonso, and G. Grandi, "Smart Charging for Electric Car-Sharing Fleets Based on Charging Duration Forecasting and Planning," MDPI Sustainability, vol.14, no.19, Oct. 2022. doi: 10.3390/su141912077.

[5] V. Sawant and P. Zambare, "DC fast charging stations for electric vehicles: A review," Energy Conversion and Economics, vol.5, no.1, pp.54-71, Feb. 2024. doi: 10.1049/enc2.12111.

[6] V. Monteiro, J. C. Ferreira, A. A. Nogueiras Melendez, C. Couto, and J. L. Afonso, "Experimental Validation of a Novel Architecture Based on a Dual-Stage Converter for Off-Board Fast Battery Chargers of Electric Vehicles," IEEE Trans. Veh. Technol., vol.67, no.2, pp.1000-1011, Feb. 2018. doi: 10.1109/TVT.2017.2755545.

[7] Y. Amry, E. Elbouchikhi, F. Le Gall, M. Ghogho, and S. El Hani, "Electric Vehicle Traction Drives and Charging Station Power Electronics: Current Status and Challenges," MDPI Energies, vol.15, no.16, Aug. 2022. doi: 10.3390/en15166037.

[8] T. J. C. Sousa, D. Pedrosa, V. Monteiro, and J. L. Afonso, "A Review on Integrated Battery Chargers for Electric Vehicles," MDPI Energies, vol.15, no.8, Apr. 2022. doi: 10.3390/en15082756.

[9] "DC-DC CONVERTERS FOR ELECTRIC VEHICLE APPLICATIQNS" IEEE Electrical Insulation Conference and Electrical Manufacturing Expo : Nashville, TN, 22-24 October 2007.

[10] Akshay Kumar Singh, Madhuri A. Chaudhari, K. S. Raja Sekhar, Rohit Kumar, " Analysis of Isolated DC-DC Converters for Electric-Vehicle (EV) Battery Charging", IEEE RESEM, 2023

[11] D. H. Kim, M. S. Kim, S. H. Nengroo, C. H. Kim, and H. J. Kim, "Llc resonant converter for lev (Light electric vehicle) fast chargers," MDPI Electronics, vol.8, no.3, Mar. 2019. doi: 10.3390/electronics8030362.

[12] M. Israr and P. Samuel, "Study and Design of DC-DC LLC Full Bridge Converter for Electric Vehicle Charging Application," IEEE ICPCES International Conference on Power, Control and Embedded Systems, 2023. doi: 10.1109/ICPCES57104.2023.10076234.

[13] C. Bhuvaneswari and R. Babu, "A review on LLC Resonant Converter," in 2016 International Conference on Computation of Power, Energy, IEEE ICCPEIC, pp-620-623, Aug. 2016. doi: 10.1109/ICCPEIC.2016.7557268.

[14] Carlos Miguel Schwarz Gonçalves Henriques, "Análise e Dimensionamento de Conversores LC e LLC Ressonante Série," MSc Dissertation, FEUP, University of Porto, 2013.

[15] H. Lei, N. Lida, N. Xiangxin, and M. Huizhuo, "Design of LLC Resonant Type Full-Bridge DC-DC Converter," Journal of Physics: Conference Series, IOP Publishing Ltd, Aug. 2021. doi: 10.1088/1742-6596/1993/1/012020.

[16] J. Zeng, G. Zhang, S. S. Yu, B. Zhang, and Y. Zhang, "LLC resonant converter topologies and industrial applications -A review," Chinese Journal of Electrical Engineering, vol.6, no.3, pp.73-84, Sep. 2020. doi: 10.23919/CJEE.2020.000021.

[17] Fariborz Musavi, Marian Craciun, Murray Edington, Wilson Eberle, and William G. Dunford, "Practical Design Considerations for a LLC Multi-Resonant DC-DC Converter in Battery Charging Applications,"IEEE APEC 2012.

[18] J. Zhao, X. Tang, H. Wu, Y. Xing, and K. Sun, "An Improved LLC Resonant Converter with Variable-Rectifier for Electric-Vehicle Charger Application; An Improved LLC Resonant Converter with Variable-Rectifier for Electric-Vehicle Charger Application," IEEE ECCE Asia 2019.

[19] J. Dudrik, P. Špánik, and N. D. Trip, "Zero-voltage and zero-current switching full-bridge DC-DC converter with auxiliary transformer," IEEE Trans. Power Electron., vol.21, no.5, pp.1328-1335, 2006. doi: 10.1109/TPEL.2006.880285.

[20] B. Lu, W. Liu, Y. Liang, F. C. Lee, and J. D. Van Wyk, "Optimal Design Methodology for LLC Resonant Converter."IEEE APEC, 2006.